

# Multimodal Knowledge Distillation for Egocentric Action Recognition Robust to Missing Modalities

Maria Santos-Villafranca <sup>\*1</sup>  
Jesus Bermudez-Cameo <sup>1</sup>

Dustin Carrión-Ojeda <sup>\*2,3</sup>  
Jose J. Guerrero <sup>1</sup>

Alejandro Perez-Yus <sup>1</sup>  
Simone Schaub-Meyer <sup>2,3</sup>

<sup>1</sup>I3A - University of Zaragoza    <sup>2</sup>IVA - TU Darmstadt    <sup>3</sup>hessian.AI

<https://visinf.github.io/KARMMA>

## Abstract

Existing methods for egocentric action recognition often rely solely on RGB videos, while additional modalities, e.g., audio, can improve accuracy in challenging scenarios. However, most prior multimodal approaches assume all modalities are available at inference, leading to significant accuracy drops, or even failure, when inputs are missing. To address this, we introduce KARMMA, a multimodal Knowledge distillation approach for egocentric Action Recognition robust to Missing Modalities that requires no modality alignment across all samples during training or inference. KARMMA distills knowledge from a multimodal teacher into a multimodal student that benefits from all available modalities while remaining robust to missing ones, making it suitable for diverse multimodal scenarios without retraining. Our student uses approximately 50 % fewer computational resources than our teacher, resulting in a lightweight and fast model. Experiments on Epic-Kitchens and Something-Something show that our student achieves competitive accuracy while significantly reducing accuracy drops under missing modality conditions.

## 1. Introduction

Egocentric vision aims to capture and interpret the world from a first-person perspective. Recently, there has been an increasing interest in this topic due to the advances in wearable technology and the rising popularity of virtual reality (VR). Egocentric vision has a wide range of applications, including assistive devices [25], human–computer interaction [3], surveillance [2], and VR gaming [6].

The release of large-scale egocentric datasets [7, 14–16, 27, 33, 47] has enabled progress on tasks such as action recognition [12, 39, 42], object recognition [1, 20, 57], localization [10, 29, 52], and others [24, 37, 46]. Compared with the exocentric (third-person) setting, egocentric video

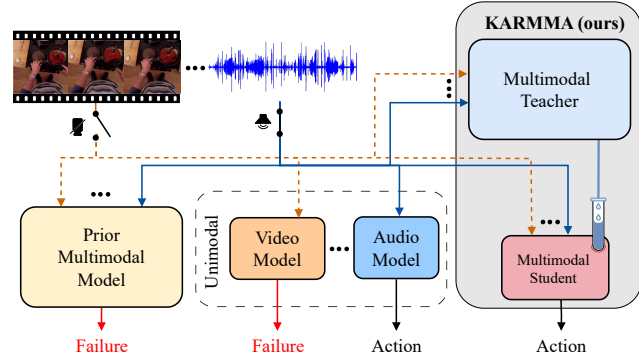


Figure 1. **KARMMA motivation.** Existing *multimodal* models for egocentric action recognition are often computationally heavy and assume that all modalities are present at inference; thus, failing when any modality is missing. Conversely, *unimodal* models are lightweight but require a separate model per modality, increasing training cost and reducing their flexibility. Therefore, we introduce KARMMA, a novel *multimodal-to-multimodal* framework that leverages all available modalities while remaining robust when any are absent, removing the need for modality-aligned data. KARMMA produces a lightweight student that runs on *any* subset of the trained modalities, offering high flexibility and resource efficiency. Solid lines indicate modalities that are present, and dashed lines those that are unavailable, e.g., because a sensor has failed.

is more challenging due to camera motion resulting in blur and frequent occlusions. To mitigate these issues, recent works have explored multimodal cues [12, 23, 26, 40, 42, 43]. However, most multimodal methods assume that every modality is present at inference time. This assumption often fails in practice because of privacy constraints or sensor malfunctions [58] (e.g., a faulty wearable camera). Moreover, multimodal architectures generally suffer significant accuracy drops when the most informative modality is missing [34], such as when RGB video is absent in egocentric action recognition.

We overcome these limitations with a multimodal frame-

work that leverages every available modality and improves robustness when modalities are missing. However, traditional multimodal models are computationally heavy because they often train large feature extractors for each modality and require aligned training data of all modalities. Instead, we propose a multimodal-to-multimodal distillation pipeline where a large teacher, built by fusing frozen, pre-trained unimodal encoders, transfers its knowledge to a lightweight student. Notably, both models can operate on any subset of modalities during training and inference, making them suitable for a wide variety of real-world applications where sensor availability is unpredictable (see Fig. 1).

**Contributions.** (1) We propose a novel multimodal-to-multimodal distillation framework for egocentric action recognition that does not require every modality to be present in every sample during training or inference. (2) Our distillation process explicitly handles missing modalities, producing a lightweight, fast, and flexible student that maintains strong accuracy with any subset of modalities while still benefiting from all modalities when available. (3) Our teacher fuses features from frozen, pre-trained unimodal encoders, removing the need to retrain them which simplifies the integration of newer encoders as they become available. (4) We introduce a fusion block with a simple parameter-free token reduction strategy that lowers computational cost without sacrificing accuracy.

## 2. Related Work

**Egocentric action recognition** has been addressed mostly using RGB video [50, 51, 55], which is the most informative modality for this task. However, several studies have shown that incorporating extra modalities, such as inertial measurements (IMUs) [53, 62], gaze [36], or audio [23], can boost accuracy, especially when video alone is ambiguous. Early multimodal research concentrated on bimodal setups, but the recent release of multimodal egocentric datasets [7, 14–16, 27, 33, 47] has encouraged the development of multimodal approaches beyond two modalities. For instance, Gong et al. [12] investigate how well models generalize to unseen modalities and to missing ones, whereas Dong et al. [8] study domain generalization under missing modality conditions. Additionally, several works [17, 42] distill a multimodal teacher into a unimodal student to improve its accuracy. In contrast, we distill knowledge from a large multimodal teacher into a compact multimodal student capable of handling missing modalities.

**Modality fusion** is commonly performed using cross-attention [40, 61] due to the success of transformer architectures, but such pairwise fusion limits scalability beyond two modalities. Contrastive objectives provide another way to fuse pairs of modalities [18, 28, 40]. For example, Lin et al. [28] introduce a contrastive loss tailored to egocen-

tric video-language alignment. Other methods pre-train modality-specific experts and then fuse their frozen features using model-agnostic mechanisms [42, 59], enabling fusion across more than two modalities. However, all these approaches assume that every modality is present at inference time. To address this, Gong et al. [12] use modality dropout during training to improve robustness to missing modalities, while Ramazanova et al. [44] add a learnable modality token that is activated only when a modality is missing. Ramazanova et al. [45] introduces a test-time adaptation approach to deal with missing modalities; however, its optimization algorithm requires a forward pass for each modality combination and only drops a fixed modality in a bi-modal setting. Our transformer-based fusion extends these works by combining modality dropout with two types of learnable tokens. The final student model is fast and can handle any subset of available modalities, no requiring additional forward passes.

**Token reduction** has been crucial for the development of fusion methods based on self-attention, as their computational cost increases quadratically with the number of input tokens [54]. To mitigate this cost, Fayyaz et al. [9] proposes a parameter-free module that prunes the attention matrix, whereas Shang et al. [48] prunes tokens by clustering them using the interquartile range scoring function [5]. Alternatives merge redundant tokens based on cosine similarity [4] or treat tokens as samples of a continuous signal and subsample accordingly [35]. Instead, we show that a very simple parameter-free strategy, averaging contiguous tokens within each modality, effectively reduces the computation of our method without sacrificing accuracy.

**Knowledge distillation** transfers the knowledge from a large teacher to a smaller student [19], and recent variants dynamically swap teacher-student roles during training [11, 60]. In multimodal settings, Radevski et al. [42] and Hatano et al. [17] improve the accuracy of a unimodal student using a multimodal teacher, while Wei et al. [56] propose a multimodal-to-multimodal distillation framework with modality dropout for classification and segmentation tasks. Building on these ideas, we introduce a novel multimodal-to-multimodal distillation framework specifically for egocentric action recognition that combines modality dropout with an additional mechanism to further enhance robustness to missing modalities.

## 3. KARMMA

This work focuses on the multimodal egocentric action recognition task, which aims to classify human actions by analyzing data from multiple egocentric modalities. Fig. 2 summarizes our proposed KARMMA framework, which distills knowledge from a large teacher into a small student.

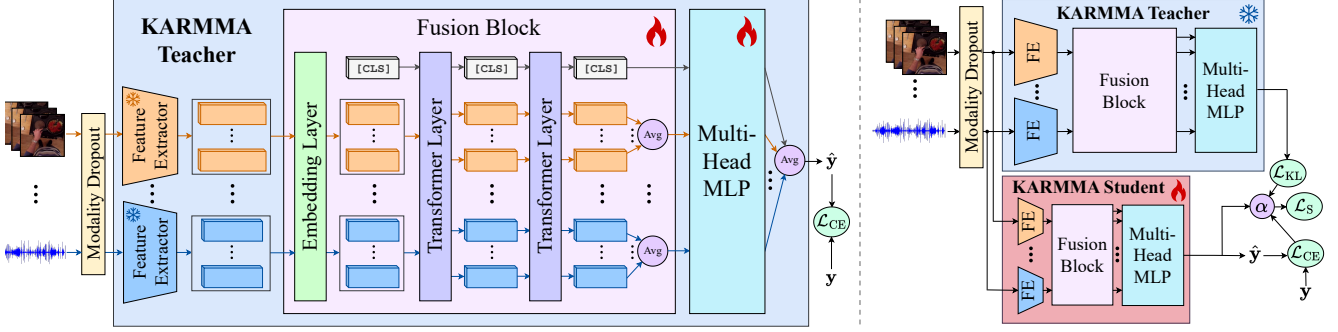


Figure 2. **KARMMA training.** *Left* (first stage): training the teacher. *Right* (second stage): distilling knowledge from the frozen teacher into the student. Both networks use modality dropout and our student includes our strategy for handling missing modalities (see Sec. 3.4) to remain robust when inputs are incomplete.

### 3.1. Problem Definition

Given an egocentric dataset with  $M$  modalities, let  $\mathbf{x}_i^j \in \mathbb{R}^{T \times D_1^j \times D_2^j \times \dots \times D_n^j}$  denote the  $i^{\text{th}}$  action sequence for the  $j^{\text{th}}$  modality, where  $T$  is the number of time-steps and  $D_1^j \times D_2^j \times \dots \times D_n^j$  are the  $n$  modality-specific spatial or spectral dimensions. For any multimodal action sequence  $\mathbf{X}_i = \{\mathbf{x}_i^1, \mathbf{x}_i^2, \dots, \mathbf{x}_i^M\}$ , the goal is to learn a model  $f$  that predicts the corresponding action  $\mathbf{y}_i$  from a set of possible actions, formulated as  $\hat{\mathbf{y}}_i = \text{argmax } \sigma(f(\mathbf{X}_i))$ , where  $\sigma(\cdot)$  denotes the softmax operator. Note that  $\mathbf{X}_i$  may contain any subset of the  $M$  modalities, so  $f$  must be robust to missing modalities. Moreover, the representation of actions  $\mathbf{y}_i$  varies across datasets. For example, in Something-Something [14], an action is a single output,  $\mathbf{y}_i = \{\text{phrase}\}$ , whereas in Epic-Kitchens [7], an action consists of multiple outputs,  $\mathbf{y}_i = \{\text{noun, verb}\}$ .

### 3.2. Teacher and Student

The architecture of both teacher and student has three components: modality-specific feature extractors (FEs), a transformer-based fusion block (FB), and a multi-head MLP (MH-MLP). A key advantage of our teacher and student is their ability to perform inference on *any* subset of the training modalities, so a single model suffices for all modality combinations. Additionally, the student uses smaller FEs and a more compact FB, which reduces memory usage and speeds up inference.

**Feature Extractors (FEs).** As noted in Sec. 3.1, the input data  $\mathbf{X}_i$  can comprise up to  $M$  modalities. Thus, to keep teacher training affordable, we use  $M$  *frozen*, pre-trained *unimodal* FEs and train only the remaining components. This approach facilitates the updating of FEs as newer encoders become available. For each modality we select an established FE available in multiple sizes, allowing the teacher to use a larger version, whereas the student uses a smaller one. When possible, student FEs are initialized with pre-trained weights and then fine-tuned.

**Fusion Block (FB).** Inspired by previous works [12, 31, 34, 38, 49], we design a transformer-based FB capable of handling an arbitrary number of input tokens and modalities. As shown in Fig. 2 (left), modality-specific tokens are first processed with an embedding layer that linearly projects them to a common dimension. These projected tokens, along with a learnable [CLS] token, pass through  $l$  transformer layers. The FB outputs  $M+1$  tokens: one averaged token per modality and the [CLS] token that aggregates cross-modal information, providing a modality-agnostic cue that remains informative when some modalities are missing.

**Multi-Head MLP (MH-MLP).** In the final stage of our framework, the  $M+1$  tokens produced by the FB are fed to a MH-MLP that consists of a shared fully connected layer followed by independent classification heads, where the number of heads matches the number of outputs required to describe an action. As explained in Sec. 3.1, actions may be described by a single output (e.g., Something-Something [14]) or by multiple outputs (e.g., Epic-Kitchens [7]). For each head, we average the  $M+1$  predictions to obtain the final output ( $f(\mathbf{X}_i)$ ).

### 3.3. Token Reduction Strategy

Since the memory requirements of our fusion block increase with every additional modality, we propose a very simple *parameter-free* token reduction strategy ( $\Theta$ -Average) that caps the number of tokens per modality w.r.t. to a chosen threshold  $\Theta$ . If a given modality feature extractor outputs  $k$  tokens, where  $k > \Theta$ , we partition the tokens into  $\Theta$  groups of  $\lfloor \frac{k}{\Theta} \rfloor$  tokens each, where the last group receives the remaining  $k \bmod \Theta$  tokens. Averaging the tokens within each group yields exactly  $\Theta$  tokens for that modality. On the other hand, if  $k \leq \Theta$ , all tokens remain unchanged. Applying our  $\Theta$ -Average to the outputs of both teacher and student feature extractors limits the number of tokens entering the fusion block, thereby lowering its computational and memory costs without adding learnable parameters.

### 3.4. KARMMA Enhancements

Our proposed KARMMA framework incorporates three main enhancements: (1) modality dropout applied to both teacher and student, (2) a novel student-side strategy for handling missing modalities, and (3) a multimodal-to-multimodal distillation scheme that boosts the accuracy of a flexible, lightweight, and fast student, eliminating the need for using a large, slow model at inference.

**Modality Dropout.** Previous works [12, 44, 56] have shown that using modality dropout during training improves robustness to missing modalities. Modality dropout works similarly to standard neuron dropout but operates at modality level, *i.e.*, it removes entire modalities with probability  $p$  while guaranteeing that at least one modality remains active. As illustrated in Fig. 2 (right), we apply modality dropout to *both* the teacher and the student, so neither network depends on the full modality set during training. This allows KARMMA to train on datasets where action sequences  $\mathbf{X}_i$  can contain different modality subsets (*i.e.*, no modality alignment needed), making our framework highly flexible and applicable to practical scenarios.

**Missing Modality Strategy.** To further enhance the robustness of the student to missing modalities, we propose a simple yet effective strategy illustrated in Fig. 3. Our strategy introduces two types of learnable tokens:

1. *Modality-specific token* ( $\check{\mathbf{t}}^m$ ): a single token per modality that helps distinguish modalities and acts similar to positional encodings.
2. *Token-specific tokens* ( $\check{\mathbf{t}}_i^m$ ): a set of  $k$  tokens for each modality that allow the model to compensate when that modality is absent.

Formally, let the feature extractor for modality  $m$  generate  $k$  tokens from the input  $\mathbf{x}_i^m$ . Then the output of the embedding layer  $\mathbf{o}_i^m$  is expressed as

$$\mathbf{o}_i^m = \begin{cases} \{\mathbf{t}_i^m + \check{\mathbf{t}}^m + \check{\mathbf{t}}_i^m\}_{i=1}^k & \text{if } m \text{ is present,} \\ \{\check{\mathbf{t}}^m + \check{\mathbf{t}}_i^m\}_{i=1}^k & \text{otherwise,} \end{cases} \quad (1)$$

where  $\mathbf{t}_i^m$  represents the  $i^{\text{th}}$  projected token for modality  $m$ .

This strategy provides rich information by combining both types of learnable tokens while keeping the input size of the fusion block unchanged, allowing the network to effectively handle any pattern of missing modalities.

**Knowledge Distillation.** As shown in Fig. 2, our KARMMA framework operates in two stages. In the first stage, we train a large multimodal teacher, whose feature extractors remain frozen, using the cross-entropy loss

$$\mathcal{L}_{\text{CE}} = -\frac{1}{N} \sum_{i=1}^N \mathbf{y}_i \cdot \log \hat{\mathbf{y}}_i^T, \quad (2)$$

where  $N$  is the number of training action sequences,  $\mathbf{y}_i$  is the ground-truth action, and  $\hat{\mathbf{y}}_i^T$  is the predicted action.

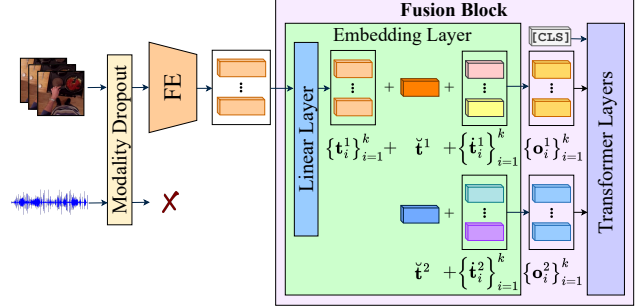


Figure 3. **Missing modality strategy.** To handle missing modalities, the embedding layer projects the tokens from the feature extractor when available. Then, it adds the learned modality token  $\check{\mathbf{t}}^m$  to all the projected tokens. Finally, a learned token  $\check{\mathbf{t}}_i^m$  is added to each individual token.

In the second stage, the trained teacher is frozen and its knowledge is distilled to a lightweight student by aligning the class probability distributions from both models via the Kullback–Leibler (KL) divergence:

$$\mathcal{L}_{\text{KL}} = \frac{1}{N} \sum_{i=1}^N \bar{\mathbf{y}}_i^T \cdot (\log \bar{\mathbf{y}}_i^T - \log \bar{\mathbf{y}}_i^S), \quad (3)$$

where  $\bar{\mathbf{y}}_i^T = \sigma(f^T(\mathbf{X}_i))$  and  $\bar{\mathbf{y}}_i^S = \sigma(f^S(\mathbf{X}_i))$  are the class probability distributions from the teacher and student, respectively. However, to prevent the student from just copying the teacher, we train it with a combination of the cross-entropy and distillation losses

$$\mathcal{L}_S = \alpha \mathcal{L}_{\text{CE}} + (1 - \alpha) \mathcal{L}_{\text{KL}}, \quad (4)$$

where  $\alpha$  balances the loss terms. The full student, including its feature extractors, is trained with this loss, resulting in a model with improved accuracy while using far less memory and delivering faster inference than the teacher.

## 4. Experiments

**Datasets.** We evaluate our KARMMA framework on two standard egocentric action recognition datasets: Epic-Kitchens-100 [7] and Something-Something V2 [14]. Epic-Kitchens includes 300 nouns and 97 verbs, with each action defined as a verb-noun pair (*e.g.*, “pick up + knife”). For this dataset, we consider three modalities: RGB video (V), optical flow (F), and audio (A). On the other hand, Something-Something contains 174 object-agnostic actions (*e.g.*, “moving [something] up”) with three modalities: V, F, and object detection annotations (D).

As in most previous works, we report results on the validation sets of both datasets, since the official test splits are not publicly available. However, we found that the Epic-Kitchens validation split contains four nouns that are absent from the training data; thus, we remove the corresponding

samples and evaluate on this *pruned* validation set. Moreover, to avoid overestimating the generalization capabilities of our method by validating and testing on the same data, we create *Epic-Kitchens*<sup>\*</sup>: a 90 % / 10 % train/val split of the original training set, reserving the pruned validation split solely for testing.<sup>1</sup>

**Implementation Details.** For the *teacher*, we use Swin-B [30] pre-trained on Kinetics-400 [22] as the feature extractor for modalities V, A, and F, and a 12-layer STLT [41] pre-trained on Action Genome [21] for D. The fusion block has an embedding dimension of 768, 2 transformer layers ( $l=2$ ), 8 attention heads, 30 % attention dropout, and 50 % modality dropout. We apply  $\Theta$ -Average token reduction with  $\Theta=300$  (see Sec. 3.3). The teacher is trained using AdamW [32] for 100 epochs with a batch size of 32, 0.05 weight decay, and gradient clipping at 1.0. The learning rate starts at  $1e^{-5}$ , warms up linearly to  $5e^{-4}$  over 10 epochs, and then follows cosine decay back to the initial value.

Unless stated otherwise, the *student* inherits the hyper-parameters of the teacher. It uses Swin-T [30] pre-trained on Kinetics-400 [22] as the feature extractor for modalities V and F, AST-T [13] for A, and a 9-layer STLT [41] for D; the latter two lack publicly available pre-trained weights and are therefore trained from scratch. The fusion block is reduced to an embedding dimension of 384, with  $l=1$ , and no attention dropout. We train the student with a batch size of 6, a weight decay of 0.01, gradient clipping at 2.0, and a peak learning rate of  $1e^{-4}$ . In Eq. (4), we set  $\alpha=0.7$ .

#### 4.1. Analysis of our KARMMA Framework

To evaluate the effectiveness of KARMMA, Tab. 1 reports the top-1 action recognition accuracy of our teacher (KARMMA<sub>T</sub>) and student (KARMMA<sub>S</sub>) models introduced in Sec. 3.2. KARMMA<sub>S</sub> incorporates the enhancements described in Sec. 3.4; thus, to isolate the contribution of each component, we compare it against two baselines: (1) Baseline uses the same architecture as KARMMA<sub>S</sub> but is trained end-to-end with cross-entropy loss and omits all KARMMA enhancements; (2) Baseline w/  $\delta$  augments Baseline with modality dropout and our missing modality strategy but no knowledge distillation.

The results in Tab. 1 show that both baselines and the student outperform the teacher across most modality combinations. Typically, in knowledge distillation, the teacher achieves better results than the student. However, in this work, the student benefits from full training. Therefore, although KARMMA<sub>S</sub> uses smaller feature extractors than KARMMA<sub>T</sub>, they are fine-tuned for multimodal egocentric action recognition, rather than kept frozen. In contrast, by keeping its feature extractors frozen, KARMMA<sub>T</sub> focuses on learning the best strategy to fuse features from different modalities. Additionally, since it also uses modality

Method	Inference Modalities	Epic-Kitchens	Epic-Kitchens <sup>*</sup>	Something-Something
Baseline		40.00	39.26	57.31
Baseline w/ $\delta$	V+F+[A/D]	<u>41.49</u>	<u>40.05</u>	<u>60.31</u>
KARMMA <sub>S</sub>		<b>43.00</b>	<b>41.98</b>	<b>62.88</b>
KARMMA <sub>T</sub>		36.44	35.84	53.51
Baseline		36.80	36.07	56.98
Baseline w/ $\delta$	V+F	<u>39.69</u>	<u>39.00</u>	<b>60.38</b>
KARMMA <sub>S</sub>		<b>41.29</b>	<b>40.42</b>	<b>58.34</b>
KARMMA <sub>T</sub>		32.96	31.99	43.14
Baseline		37.48	36.60	40.03
Baseline w/ $\delta$	V+[A/D]	<u>39.36</u>	<u>37.76</u>	<u>53.04</u>
KARMMA <sub>S</sub>		<b>40.84</b>	<b>40.10</b>	<b>59.35</b>
KARMMA <sub>T</sub>		33.79	33.44	49.89
Baseline		5.49	6.84	37.35
Baseline w/ $\delta$	F+[A/D]	<u>27.09</u>	<u>27.21</u>	<u>50.78</u>
KARMMA <sub>S</sub>		<b>30.36</b>	<b>28.24</b>	<b>53.96</b>
KARMMA <sub>T</sub>		20.44	19.95	40.62
Baseline		32.10	32.50	39.91
Baseline w/ $\delta$	V	<u>37.84</u>	<u>36.48</u>	<b>53.02</b>
KARMMA <sub>S</sub>		<b>38.85</b>	<b>38.37</b>	<b>51.97</b>
KARMMA <sub>T</sub>		29.44	29.34	33.80
Baseline		2.58	4.73	36.50
Baseline w/ $\delta$	F	<u>25.64</u>	<u>26.01</u>	<b>50.97</b>
KARMMA <sub>S</sub>		<b>27.28</b>	<b>26.06</b>	<b>47.24</b>
KARMMA <sub>T</sub>		15.51	15.70	23.82
Baseline		2.05	2.25	0.07
Baseline w/ $\delta$	[A/D]	6.23	6.44	1.21
KARMMA <sub>S</sub>		<u>8.17</u>	<u>7.53</u>	<b>37.95</b>
KARMMA <sub>T</sub>		<b>9.38</b>	<b>9.11</b>	29.40

Table 1. **Analysis of KARMMA under different modality combinations.** “KARMMA<sub>T</sub>” and “KARMMA<sub>S</sub>” denote our teacher and student, respectively (see Sec. 3.2). The “Baseline” uses the same architecture as “KARMMA<sub>S</sub>” but is trained end-to-end with cross-entropy loss and without the KARMMA enhancements (see Sec. 3.4), whereas “Baseline w/  $\delta$ ” incorporates modality dropout and our missing modality strategy. “V,” “F,” “A,” and “D” refer to RGB video, optical flow, audio, and object detection annotations, respectively, and “[A/D]” indicates that either audio or object detection is used. We report top-1 action recognition accuracy (%) on all datasets. The “Epic-Kitchens” column reports results on our custom split (see Sec. 4). Blue highlights our final teacher and student. **Bold** and underlined values indicate the best and second-best results.

dropout, it learns to handle missing modalities. Consequently, transferring its knowledge to KARMMA<sub>S</sub> yields absolute gains (relative gains in parentheses) of 3.00 % (7.5 %), 2.72 % (6.9 %), and 5.57 % (9.7 %) over the Baseline when all modalities are present on the Epic-Kitchens, Epic-Kitchens<sup>\*</sup>, and Something-Something datasets, respectively. Additionally, the results on Epic-Kitchens<sup>\*</sup> closely match those on the original dataset, demonstrating the generalization ability of our KARMMA framework.

Tab. 1 also shows that the highest accuracy is achieved when all modalities are available, confirming that our model effectively leverages multimodal information. The results

<sup>1</sup>The Epic-Kitchens<sup>\*</sup> split will be released with our code.

also confirm that RGB video is the most informative signal, while audio and object detection annotations contribute the least. Consequently, switching from V+[A/D] to F+[A/D] leads to a significant accuracy drop across all models. This drop is even more pronounced in unimodal settings that rely solely on [A/D]. However, the drop is more severe for the Baseline model, indicating that modality dropout and our missing modality strategy help mitigate over-reliance on the most informative modality.

Since KARMMA<sub>S</sub> outperforms both baselines across most modality combinations and datasets, it demonstrates that while a model can be trained to handle missing modalities (Baseline w/  $\delta$ ), incorporating our knowledge distillation further enhances both accuracy and robustness to missing modalities. This improvement is particularly evident on Something-Something, where KARMMA<sub>S</sub> achieves an absolute accuracy gain of 36.74 % ( $\approx 3000$  % relative) over Baseline w/  $\delta$  when only object detection annotations (D) are used. For Epic-Kitchens, the gain is smaller at 1.94 % (31 % relative), but it still represents a substantial improvement over Baseline w/  $\delta$  when only audio (A) is used. The large difference in gains between the two datasets may be due to audio being less informative than object detection annotations, which provide spatial and dimensional information about the objects involved in the action.

Although Tab. 1 demonstrates that our student can effectively handle missing modalities, it only considers scenarios where entire modalities are absent at inference time. In contrast, real-world situations may involve dynamically missing modalities. To simulate such conditions, Fig. 4 reports the action recognition accuracy of the two baselines and our student as the probability of dropping each modality increases from 0 % to 90 % during inference. These results show that the Baseline model is highly sensitive: missing one or more modalities in just 10% of the samples already reduces accuracy by roughly 5 % on both datasets, and increasing this probability to 90 % leads to absolute drops of about 27 % and 32 % for Epic-Kitchens and Something-Something, respectively. Incorporating modality dropout and our missing modality strategy enhances robustness, as Baseline w/  $\delta$  exhibits a significantly smaller accuracy drop than the Baseline. Moreover, our distillation pipeline consistently improves the accuracy of KARMMA<sub>S</sub>, yielding absolute gains (relative gains in parentheses) of approximately 2 % (9 %) and 12 % (34 %) over Baseline w/  $\delta$  in the 90% missing modality setting for Epic-Kitchens and Something-Something, respectively.

## 4.2. Comparison With the State of the Art

Since KARMMA is inspired by Radevski et al. [42], which is the current state-of-the-art (SOTA) method in multimodal-to-unimodal distillation for egocentric action recognition, Tab. 2 presents a comparison between our ap-

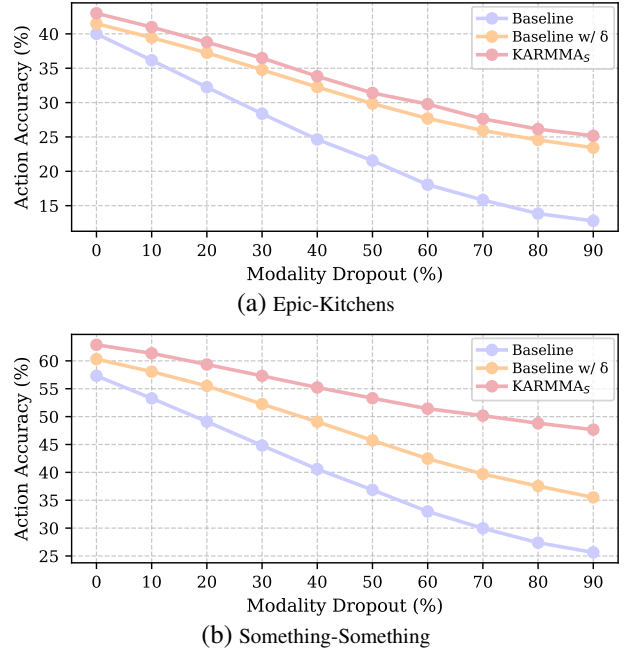


Figure 4. **Impact of missing modalities at inference.** The “Baseline” uses the same architecture as our student “KARMMA<sub>S</sub>” (see Sec. 3.2) but is trained end-to-end with cross-entropy loss and without the KARMMA enhancements (see Sec. 3.4), whereas “Baseline w/  $\delta$ ” incorporates modality dropout and our missing modality strategy.

proach and theirs on the Epic-Kitchens dataset. For a fair comparison, we report two versions of our model: a unimodal (RGB video only) student (KARMMA<sub>V</sub>), and our full multimodal student (KARMMA<sub>S</sub>).

The top part of Tab. 2 shows that our KARMMA<sub>V</sub> achieves slightly lower accuracy than the student of Radevski et al. [42]. However, our KARMMA<sub>V</sub> uses a teacher with approximately 7.5 times fewer trainable parameters, as our teacher does not fine-tune its feature extractors. Moreover, both models are limited to performing inference with RGB video only. This constraint implies that a separate student must be trained for each input modality or modality combination, which can be impractical in resource-constrained scenarios.

The bottom part of Tab. 2 shows how our KARMMA<sub>S</sub> overcomes this limitation, as it can perform inference with various modality combinations, unlike the unimodal students. Since KARMMA<sub>S</sub> is designed to handle and benefit from multiple modalities, its accuracy on RGB video alone is slightly lower than that of the unimodal models, which are optimized specifically for this modality. However, when all modalities are available, KARMMA<sub>S</sub> outperforms the student of Radevski et al. [42] by 1.19 % (2.9 % relative).

Additionally, when performing inference on a single modality, all models have a similar computational cost, making our multimodal student just as efficient while offer-

Method	Student Train. Mods.	Student Infer. Mods.	Flexible Mod. Inference	Teacher Train. Params. (M)	Student Train. Params. (M)	Action Acc. (%)	GFLOPs
Radevski et al. [42]	V	V	x	84.65	<b>28.21</b>	41.81	<b>175</b>
KARMMAv			x	<b>11.25</b>	<u>29.64</u>	40.84	<u>176</u>
KARMMAs	V+F+A	V	✓	<b>11.25</b>	65.15	38.85	<b>176</b>
KARMMAs	V+F+A	V+F+A	✓	<b>11.25</b>	65.15	<b>43.00</b>	358

Table 2. **Comparison with the SOTA multimodal-to-unimodal distillation approach for egocentric action recognition.** All methods distill knowledge from a multimodal teacher trained on RGB video (V), optical flow (F), and audio (A). “KARMMAv” refers to a unimodal version of our multimodal student (“KARMMAs”). Results for Radevski et al. [42] are computed using their publicly available student checkpoint. Blue highlights our final student. **Bold** and underline values indicate the best and second-best results.

ing the added flexibility of supporting multiple modalities. Therefore, KARMMAs can be used across diverse multimodal scenarios, leveraging all available modalities while maintaining robustness in the presence of missing ones.

### 4.3. Ablation Studies

All ablations are performed on the Epic-Kitchens-100 [7] dataset with models trained for 50 epochs (*cf.*, 100 in the main experiments). Additional ablations are included in the [Appendix](#).

**KARMMAs Enhancements.** The results in Tab. 3 show that applying modality dropout improves the noun, verb and action accuracy of the Baseline. Adding our proposed strategy for handling missing modalities further improves verb and action accuracy. Knowledge distillation yields the largest gains across all metrics, and training the student for 100 epochs provides an additional boost. These results demonstrate that our KARMMAs enhancements not only increase the robustness to missing modalities (see Tab. 1 and Fig. 4) but also enhance the overall accuracy.

**Knowledge Distillation.** The balance between teacher supervision (knowledge distillation) and task supervision (cross-entropy) is controlled by the coefficient  $\alpha$  in Eq. (4). Therefore, Tab. 4 reports the student noun, verb and action accuracy for different  $\alpha$  values. The results highlight the importance of properly balancing teacher and task supervision: no reliance on the teacher ( $\alpha=1.0$ ) fails to leverage the additional guidance it provides, while too much reliance ( $\alpha=0.1$ ) leads to overfitting to its outputs and a drop in accuracy. The optimal balance is achieved with  $\alpha=0.7$ , yielding an absolute action accuracy gain of 1.81 % (4.5 % relative) over training without distillation ( $\alpha=1.0$ ).

**Token Reduction.** Tab. 5 shows the impact of token reduction in the fusion block of our teacher. Using all tokens yields the highest accuracy, but our parameter-free strategy ( $\Theta$ -Average) with  $\Theta=300$  achieves the best accuracy-efficiency trade-off: it reduces memory usage by 11.63 GB (81.45 % relative) and lowers GFLOPs, with only a 0.27 % absolute drop in accuracy. In more constrained scenarios, a smaller threshold ( $\Theta=100$ ) further reduces

Enhancement	Noun Acc. (%)	Verb Acc. (%)	Action Acc. (%)
Baseline	50.08	64.74	38.94
+ Modality dropout	51.30	65.22	39.82
+ Missing modality strategy	50.60	65.61	39.87
+ Knowledge distillation	<u>53.05</u>	<u>67.24</u>	<u>41.68</u>
+ Longer training	<b>54.80</b>	<b>67.65</b>	<b>43.00</b>

Table 3. **Analysis of the KARMMAs enhancements.** The “Baseline” uses the same architecture as our student (see Sec. 3.2) but is trained end-to-end with cross-entropy loss and without the KARMMAs enhancements (see Sec. 3.4). “Longer training” denotes 100 training epochs. Blue highlights our final student. **Bold** and underline values indicate the best and second-best results.

$\alpha$	Noun Acc. (%)	Verb Acc. (%)	Action Acc. (%)
1.0	50.60	65.61	39.87
0.7	<b>53.05</b>	<b>67.24</b>	<b>41.68</b>
0.4	<u>52.03</u>	<u>66.07</u>	<u>40.17</u>
0.1	49.98	64.51	37.82

Table 4. **Impact of knowledge distillation.** The “ $\alpha$ ” column corresponds to the value used in Eq. (4) that balances the cross-entropy and distillation losses. Blue highlights the value used in our final student. **Bold** and underline values indicate the best and second-best results.

Token Reduction	# of Tokens per Mod.	GFLOPs	Mem. Usage of FB (GB)	Action Acc. (%)
None	785	1759	14.28	<b>35.26</b>
$\Theta$ -Average	500	1725	6.35	34.76
$\Theta$ -Average	<u>300</u>	<u>1707</u>	<u>2.65</u>	<u>34.99</u>
$\Theta$ -Average	<b>100</b>	<b>1693</b>	<b>0.50</b>	32.62

Table 5. **Effect of token reduction.** “None” keeps all tokens, while “ $\Theta$ -Average” applies our proposed strategy (see Sec. 3.3). Memory usage refers to the average GPU memory consumed by the fusion block during training. The top-1 action recognition accuracy is computed using our teacher, “KARMMAt”. Blue highlights the configuration used in our final teacher and student. **Bold** and underline values indicate the best and second-best results.

computational cost while maintaining competitive accuracy.

**Modality Dropout.** During training we apply different modality dropout rates and evaluate their impact at inference. Fig. 5 reports the resulting action accuracy across various modality combinations, and Tab. 6 summarizes these results using three metrics: average action accuracy, average relative drop compared to the full-modality setting (V+F+A), and average rank. A 50 % dropout rate achieves the best trade-off, yielding an absolute accuracy gain of 8.15 % (50.7 % relative) and a 25.42 % absolute reduction in relative drop (41.4 % relative) compared to no dropout. These results highlight the importance of selecting an appropriate dropout rate: too high rates ( $\geq 75\%$ ) degrade overall accuracy, while too low rates ( $\leq 25\%$ ) fail to build sufficient robustness, resulting in larger accuracy drops when modalities are missing.

**Resource Efficiency.** Fig. 6 compares the average memory usage and GFLOPs of the teacher and student at inference across different modality combinations. The results show that, in all cases, our KARMMA student reduces memory consumption by approximately 50 % and significantly lowers GFLOPs, resulting in a lightweight model with fast inference. The largest savings occur when only audio is used, as the student processes it with an AST-T [13], which is significantly smaller than the Swin-T [30] used for RGB video and optical flow.

## 5. Conclusions

In this work, we presented *KARMMA*, a novel multimodal-to-multimodal distillation framework for egocentric action recognition that requires no modality alignment across samples during training or inference. The resulting student is lightweight, fast, and benefits from the availability of multiple modalities while remaining robust to missing ones. Unlike unimodal models, our KARMMA student supports *any* combination of the training modalities without retraining, making it well-suited to real-world multimodal scenarios.

Our framework also reduces training costs by using frozen pre-trained unimodal feature extractors for the teacher, which simplifies the integration of newer extractors as they become available. Additionally, our simple parameter-free token reduction strategy improves computational efficiency without sacrificing accuracy.

Overall, KARMMA outperforms the state-of-the-art multimodal-to-unimodal distillation method for egocentric action recognition, achieving higher accuracy while being parameter- and GFLOPs-efficient. Future work could explore the generalization of KARMMA for exocentric datasets and additional modalities.

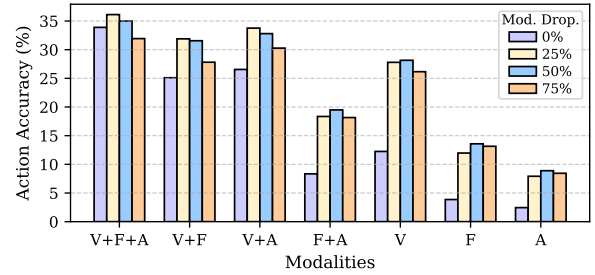


Figure 5. **Impact of modality dropout rate during training.** Each bar shows the top-1 action recognition accuracy of our teacher (see Sec. 3.2) trained with a specific modality dropout rate and evaluated across different modality combinations. “V,” “F,” and “A” refer to RGB video, optical flow, and audio, respectively.

Modality Dropout (%)	Average Accuracy (%)	Average Relative Drop (%)	Average Rank
0	16.06	61.37	3.86
25	<u>23.97</u>	39.24	<u>1.86</u>
50	<b>24.21</b>	<u>35.95</u>	<b>1.43</b>
75	22.27	<u>35.28</u>	2.86

Table 6. **Summary of the impact of modality dropout rate during training.** “Average Accuracy” refers to the mean action accuracy across all modality combinations. “Average Relative Drop” indicates the mean relative accuracy drop compared to the full-modality setting (V+F+A). “Average Rank” is the mean rank across modality combinations. All values are derived from Fig. 5. Blue highlights the modality dropout rate used in our final teacher and student. **Bold** and underline values indicate the best and second-best results.

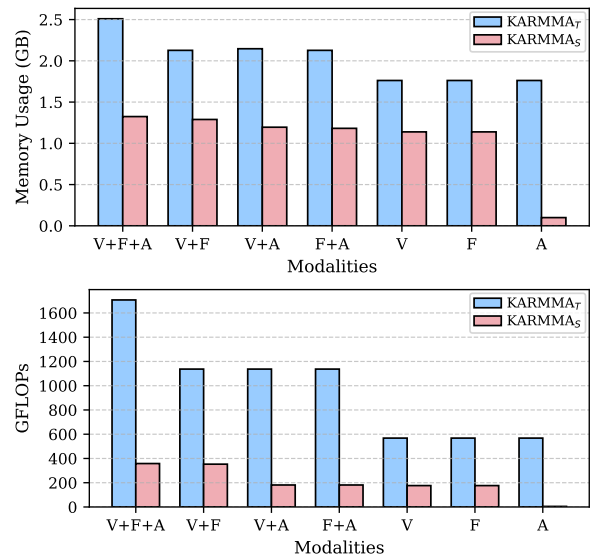


Figure 6. **Resource efficiency of KARMMA student.** “KARMMA<sub>T</sub>” and “KARMMA<sub>S</sub>” denote our teacher and student, respectively (see Sec. 3.2). The top figure compares their average GPU memory usage for different modality combinations, while the bottom figure compares their GFLOPs, both measured at inference. “V,” “F,” and “A” refer to RGB video, optical flow, and audio, respectively.

## Acknowledgments

This work was supported by projects PID2021-125209OB-I00 and TED2021-129410B-I00, (MCIN/AEI/10.13039/501100011033 and FEDER/UE and NextGenerationEU/PRTR), DGA 2022-2026 grant and Grant SMT Erasmus+, project 2022-1-ES01-KA131-HED-000065592 funded by Campus Iberus. The project has also been funded by the Hessian Ministry of Science and Research, Arts and Culture (HMWK) through the project “The Third Wave of Artificial Intelligence – 3AI”. The work was further supported by the Deutsche Forschungsgemeinschaft (German Research Foundation, DFG) under Germany’s Excellence Strategy (EXC 3057/1 “Reasonable Artificial Intelligence”, Project No. 533677015).

## References

[1] Peri Akiva, Jing Huang, Kevin J. Liang, Rama Kovvuri, Xingyu Chen, Matt Feiszli, Kristin Dana, and Tal Hassner. Self-supervised object detection from egocentric videos. In *ICCV*, pages 5225–5237, 2023. 1

[2] Shervin Ardesir and Ali Borji. Integrating egocentric videos in top-view surveillance videos: Joint identification and temporal alignment. In *ECCV*, pages 300–317, 2018. 1

[3] Md Mushfiqur Azam and Kevin Desai. A survey on 3D egocentric human pose estimation. In *CVPR*, pages 1643–1654, 2024. 1

[4] Daniel Bolya, Cheng-Yang Fu, Xiaoliang Dai, Peizhao Zhang, Christoph Feichtenhofer, and Judy Hoffman. Token merging: Your ViT but faster. In *ICLR*, 2023. 2

[5] Azzedine Boukerche, Lining Zheng, and Omar Alfandi. Outlier detection: Methods, models, and classification. *ACM Comput. Surv.*, 53(3):1–37, 2020. 2

[6] Jianchun Chen, Jian Wang, Yinda Zhang, Rohit Pandey, Thabo Beeler, Marc Habermann, and Christian Theobalt. EgoAvatar: Egocentric view-driven and photorealistic full-body avatars. In *SIGGRAPH*, pages 1–11, 2024. 1

[7] Dima Damen, Hazel Doughty, Giovanni Maria Farinella, et al. Scaling egocentric vision: The EPIC-KITCHENS dataset. In *ECCV*, pages 720–736, 2018. 1, 2, 3, 4, 7, i, ii

[8] Hao Dong, Ismail Nejjar, Han Sun, Eleni N. Chatzi, and Olga Fink. SimMMDG: A simple and effective framework for multi-modal domain generalization. In *NeurIPS*, 2023. 2

[9] Mohsen Fayyaz, Soroush Abbasi Koohpayegani, Farnoush Rezaei Jafari, Sunando Sengupta, Hamid Reza Vaezi Joze, Eric Sommerlade, Hamed Pirsavash, and Jürgen Gall. Adaptive token sampling for efficient vision transformers. In *ECCV*, pages 396–414, 2022. 2

[10] Antonino Furnari, Giovanni Maria Farinella, and Sebastiano Battiato. Temporal segmentation of egocentric videos to highlight personal locations of interest. In *ECCVW*, pages 474–489, 2016. 1

[11] Nuno Cruz Garcia, Sarah Adel Bargal, Vitaly Ablavsky, Pietro Morerio, Vittorio Murino, and Stan Sclaroff. Distillation multiple choice learning for multimodal action recognition. In *WACV*, pages 2754–2763, 2021. 2

[12] Xinyu Gong, Sreyas Mohan, Naina Dhingra, Jean-Charles Bazin, Yilei Li, Zhangyang Wang, and Rakesh Ranjan. MMG-Ego4D: Multimodal generalization in egocentric action recognition. In *CVPR*, pages 6481–6491, 2023. 1, 2, 3, 4

[13] Yuan Gong, Yu-An Chung, and James Glass. AST: Audio spectrogram transformer. In *Interspeech*, pages 571–575, 2021. 5, 8

[14] Raghav Goyal, Samira Ebrahimi Kahou, Vincent Michalski, et al. The “something something” video database for learning and evaluating visual common sense. In *ICCV*, pages 5842–5850, 2017. 1, 2, 3, 4

[15] Kristen Grauman, Andrew Westbury, Eugene Byrne, et al. Ego4d: Around the world in 3,000 hours of egocentric video. In *CVPR*, pages 18995–19012, 2022.

[16] Kristen Grauman, Andrew Westbury, Lorenzo Torresani, et al. Ego-Exo4D: Understanding skilled human activity from first-and third-person perspectives. In *CVPR*, pages 19383–19400, 2024. 1, 2

[17] Masashi Hatano, Ryo Hachiuma, Ryo Fujii, and Hideo Saito. Multimodal cross-domain few-shot learning for egocentric action recognition. In *ECCV*, pages 182–199, 2024. 2

[18] Bo He, Jun Wang, Jielin Qiu, Trung Bui, Abhinav Shrivastava, and Zhaowen Wang. Align and attend: Multimodal summarization with dual contrastive losses. In *CVPR*, pages 14867–14878, 2023. 2

[19] Geoffrey E. Hinton, Oriol Vinyals, and Jeffrey Dean. Distilling the knowledge in a neural network. *arXiv:1503.02531 [stat.ML]*, 2015. 2

[20] Mingzhen Huang, Xiaoxing Li, Jun Hu, Honghong Peng, and Siwei Lyu. Tracking multiple deformable objects in egocentric videos. In *CVPR*, pages 1461–1471, 2023. 1

[21] Jingwei Ji, Ranjay Krishna, Li Fei-Fei, and Juan Carlos Niebles. Action genome: Actions as compositions of spatio-temporal scene graphs. In *CVPR*, pages 10236–10247, 2020. 5

[22] Will Kay, João Carreira, Karen Simonyan, Brian Zhang, Chloe Hillier, Sudheendra Vijayanarasimhan, Fabio Viola, Tim Green, Trevor Back, Paul Natsev, Mustafa Suleyman, and Andrew Zisserman. The kinetics human action video dataset. *arXiv:1705.06950 [cs.CV]*, 2017. 5

[23] Evangelos Kazakos, Jaesung Huh, Arsha Nagrani, Andrew Zisserman, and Dima Damen. With a little help from my temporal context: Multimodal egocentric action recognition. In *BMVC*, page 268, 2021. 1, 2

[24] Bolin Lai, Miao Liu, Fiona Ryan, and James M. Rehg. In the eye of transformer: Global-local correlation for egocentric gaze estimation. *Int. J. Comput. Vision*, 132(3):854–871, 2024. 1

[25] Kyungjun Lee, Abhinav Shrivastava, and Hernisa Kacorri. Hand-priming in object localization for assistive egocentric vision. In *WACV*, pages 3411–3421, 2020. 1

[26] Yin Li, Zhefan Ye, and James M. Rehg. Delving into egocentric actions. In *CVPR*, pages 287–295, 2015. 1

[27] Yin Li, Miao Liu, and James M. Rehg. In the eye of beholder: Joint learning of gaze and actions in first person video. In *ECCV*, pages 639–655, 2018. 1, 2

[28] Kevin Qinghong Lin, Jinpeng Wang, Mattia Soldan, et al. Egocentric video-language pretraining. In *NeurIPS*, 2022. 2

[29] Miao Liu, Lingni Ma, Kiran Somasundaram, Yin Li, Kristen Grauman, James M. Rehg, and Chao Li. Egocentric activity recognition and localization on a 3D map. In *ECCV*, pages 621–638, 2022. 1

[30] Ze Liu, Yutong Lin, Yue Cao, Han Hu, Yixuan Wei, Zheng Zhang, Stephen Lin, and Baining Guo. Swin transformer: Hierarchical vision transformer using shifted windows. In *ICCV*, pages 10012–10022, 2021. 5, 8

[31] Zecheng Liu, Jia Wei, Rui Li, and Jianlong Zhou. SFusion: Self-attention based N-to-one multimodal fusion block. In *MICCAI*, pages 159–169, 2023. 3

[32] Ilya Loshchilov and Frank Hutter. Decoupled weight decay regularization. In *ICLR*, 2019. 5

[33] ZhaoYang Lv, Nicholas Charron, Pierre Moulon, et al. Aria everyday activities dataset. *arXiv:2402.13349 [cs.CV]*, 2024. 1, 2

[34] Mengmeng Ma, Jian Ren, Long Zhao, Davide Testuggine, and Xi Peng. Are multimodal transformers robust to missing modality? In *CVPR*, pages 18177–18186, 2022. 1, 3

[35] Dmitrii Marin, Jen-Hao Rick Chang, Anurag Ranjan, Anish Prabhu, Mohammad Rastegari, and Oncel Tuzel. Token pooling in vision transformers for image classification. In *WACV*, pages 12–21, 2023. 2

[36] Kyle Min and Jason J. Corso. Integrating human gaze into attention for egocentric activity recognition. In *WACV*, pages 1069–1078, 2021. 2

[37] Lorenzo Mur-Labadia, Jose J. Guerrero, and Ruben Martinez-Cantin. Multi-label affordance mapping from egocentric vision. In *ICCV*, pages 5238–5249, 2023. 1

[38] Arsha Nagrani, Shan Yang, Anurag Arnab, Aren Jansen, Cordelia Schmid, and Chen Sun. Attention bottlenecks for multimodal fusion. In *NeurIPS*, pages 14200–14213, 2021. 3, i, ii

[39] Chiara Plizzari, Mirco Planamente, Gabriele Goleto, Marco Cannici, Emanuele Gusso, Matteo Matteucci, and Barbara Caputo. E<sup>2</sup>(GO)MOTION: Motion augmented event stream for egocentric action recognition. In *CVPR*, pages 19935–19947, 2022. 1

[40] Shraman Pramanick, Yale Song, Sayan Nag, Kevin Qinghong Lin, Hardik Shah, Mike Zheng Shou, Rama Chellappa, and Pengchuan Zhang. EgoVLPv2: Egocentric video-language pre-training with fusion in the backbone. In *ICCV*, pages 5285–5297, 2023. 1, 2

[41] Gorjan Radenovski, Marie-Francine Moens, and Tinne Tuytelaars. Revisiting spatio-temporal layouts for compositional action recognition. In *BMVC*, 2021. 5

[42] Gorjan Radenovski, Dusan Grujicic, Matthew Blaschko, Marie-Francine Moens, and Tinne Tuytelaars. Multimodal distillation for egocentric action recognition. In *ICCV*, pages 5213–5224, 2023. 1, 2, 6, 7

[43] Alec Radford, Jong Wook Kim, Chris Hallacy, et al. Learning transferable visual models from natural language supervision. In *ICML*, pages 8748–8763, 2021. 1

[44] Merey Ramazanova, Alejandro Pardo, Humam Alwassel, and Bernard Ghanem. Exploring missing modality in multi-modal egocentric datasets. In *CVPRW*, pages 75–85, 2025. 2, 4

[45] Merey Ramazanova, Alejandro Pardo, Bernard Ghanem, and Motasem Alfarrar. Test-time adaptation for combating missing modalities in egocentric videos. In *ICLR*, 2025. 2

[46] Fiona Ryan, Hao Jiang, Abhinav Shukla, James M. Rehg, and Vamsi Krishna Ithapu. Egocentric auditory attention localization in conversations. In *CVPR*, pages 14663–14674, 2023. 1

[47] Fadime Sener, Dibyadip Chatterjee, Daniel Shelekov, Kun He, Dipika Singhania, Robert Wang, and Angela Yao. Assembly101: A large-scale multi-view video dataset for understanding procedural activities. In *CVPR*, pages 21096–21106, 2022. 1, 2

[48] Yuzhang Shang, Mu Cai, Bingxin Xu, Yong Jae Lee, and Yan Yan. LLava-PruMerge: Adaptive token reduction for efficient large multimodal models. *arXiv:2403.15388 [cs.CV]*, 2024. 2

[49] Tim Siebert, Kai Norman Clasen, Mahdyar Ravanbakhsh, and Begüm Demir. Multi-modal fusion transformer for visual question answering in remote sensing. *arXiv:2210.04510 [cs.CV]*, 2022. 3

[50] Gunnar A. Sigurdsson, Abhinav Gupta, Cordelia Schmid, Ali Farhadi, and Karteek Alahari. Actor and observer: Joint modeling of first and third-person videos. In *CVPR*, pages 7396–7404, 2018. 2

[51] Swathikiran Sudhakaran, Sergio Escalera, and Oswald Lanz. Learning to recognize actions on objects in egocentric video with attention dictionaries. *IEEE T. Pattern Anal. Mach. Intell.*, 45(6):6674–6687, 2023. 2

[52] Tamas Suveges and Stephen McKenna. Egomap: Hierarchical first-person semantic mapping. In *ICPR*, pages 348–363, 2021. 1

[53] Shuhan Tan, Tushar Nagarajan, and Kristen Grauman. EgoDistill: Egocentric head motion distillation for efficient video understanding. In *NeurIPS*, pages 33485–33498, 2023. 2

[54] Ashish Vaswani, Noam Shazeer, Niki Parmar, Jakob Uszkoreit, Llion Jones, Aidan N. Gomez, Łukasz Kaiser, and Illia Polosukhin. Attention is all you need. In *NIPS*, pages 5998–6008, 2017. 2

[55] Huiyu Wang, Mitesh Kumar Singh, and Lorenzo Torresani. Ego-Only: Egocentric action detection without exocentric transferring. In *ICCV*, pages 5250–5261, 2023. 2

[56] Shicai Wei, Chunbo Luo, and Yang Luo. MMA-Net: Margin-aware distillation and modality-aware regularization for incomplete multimodal learning. In *CVPR*, pages 20039–20049, 2023. 2, 4

[57] Jay Zhangjie Wu, David Junhao Zhang, Wynne Hsu, Mengmi Zhang, and Mike Zheng Shou. Label-efficient online continual object detection in streaming video. In *ICCV*, pages 19246–19255, 2023. 1

[58] Renjie Wu, Hu Wang, Hsiang-Ting Chen, and Gustavo Carneiro. Deep multimodal learning with missing modality: A survey. *arXiv:2409.07825 [cs.CV]*, 2024. 1

- [59] Xuehan Xiong, Anurag Arnab, Arsha Nagrani, and Cordelia Schmid. M&M mix: A multimodal multiview transformer ensemble. *arXiv:2206.09852 [cs.CV]*, 2022. [2](#)
- [60] Lehan Yang and Kele Xu. Cross modality knowledge distillation for multi-modal aerial view object classification. In *CVPR*, pages 382–387, 2021. [2](#)
- [61] Jiaming Zhang, Huayao Liu, Kailun Yang, Xinxin Hu, Ruiping Liu, and Rainer Stiefelhagen. CMX: Cross-modal fusion for RGB-X semantic segmentation with transformers. *IEEE T. Intell. Transp. Syst.*, 24(12):14679–14694, 2023. [2](#)
- [62] Mingfang Zhang, Yifei Huang, Ruicong Liu, and Yoichi Sato. Masked video and body-worn IMU autoencoder for egocentric action recognition. In *ECCV*, pages 312–330, 2024. [2](#)

## Appendix

This appendix presents additional ablation studies for KARMMA, our multimodal Knowledge distillation framework for egocentric **Action Recognition** robust to **Missing ModAlities**. Sec. A compares strategies for handling inputs with missing modalities. Sec. B contrasts two approaches for fusing multimodal features. Sec. C evaluates the contribution of the [CLS] token alongside modality tokens. Sec. D tests the generalization capabilities of our student to unseen environments. All experiments use the pruned Epic-Kitchens-100 [7] validation set described in Sec. 4, with each model trained for 50 epochs (*cf.*, 100 in the main experiments). Finally, Sec. E discusses the limitations of our KARMMA framework.

### A. Missing Modality Strategies

In addition to modality dropout, our KARMMA student incorporates an explicit strategy to enhance robustness when one or more modalities are absent. Let the feature extractor for modality  $m$  output  $k$  tokens for a given input  $\mathbf{x}_i^m$ , which are then processed by the embedding layer to produce  $k$  projected tokens  $\mathbf{o}_i^m = \{\mathbf{t}_i^m\}_{i=1}^k$ . We compare four strategies, detailed below.

**Single Learnable Modality Token.** Each modality has a single learnable token  $\check{\mathbf{t}}^m$ :

$$\mathbf{o}_i^m = \begin{cases} \{\mathbf{t}_i^m + \check{\mathbf{t}}^m\}_{i=1}^k & \text{if } m \text{ is present,} \\ \{\check{\mathbf{t}}^m\}_{i=1}^k & \text{otherwise.} \end{cases} \quad (5)$$

This strategy results in  $k$  tokens when the modality is present but only one when it is missing.

**Replicated Learnable Modality Token.** The same learned modality token  $\check{\mathbf{t}}^m$  is replicated to preserve sequence length:

$$\mathbf{o}_i^m = \begin{cases} \{\mathbf{t}_i^m + \check{\mathbf{t}}^m\}_{i=1}^k & \text{if } m \text{ is present,} \\ \{\check{\mathbf{t}}^m\}_{i=1}^k, & \text{otherwise.} \end{cases} \quad (6)$$

**Learnable Tokens per Modality.** Each modality has  $k$  learnable tokens  $\check{\mathbf{t}}_i^m$ :

$$\mathbf{o}_i^m = \begin{cases} \{\mathbf{t}_i^m + \check{\mathbf{t}}_i^m\}_{i=1}^k & \text{if } m \text{ is present,} \\ \{\check{\mathbf{t}}_i^m\}_{i=1}^k & \text{otherwise.} \end{cases} \quad (7)$$

**Combined Learnable Modality and Token-Specific Tokens.** Each modality uses a learnable modality token  $\check{\mathbf{t}}^m$  and  $k$  learnable tokens  $\check{\mathbf{t}}_i^m$ :

$$\mathbf{o}_i^m = \begin{cases} \{\mathbf{t}_i^m + \check{\mathbf{t}}^m + \check{\mathbf{t}}_i^m\}_{i=1}^k & \text{if } m \text{ is present,} \\ \{\check{\mathbf{t}}^m + \check{\mathbf{t}}_i^m\}_{i=1}^k & \text{otherwise.} \end{cases} \quad (8)$$

Here,  $\check{\mathbf{t}}^m$  provides coarse modality information, while  $\check{\mathbf{t}}_i^m$  preserve fine-grained token details.

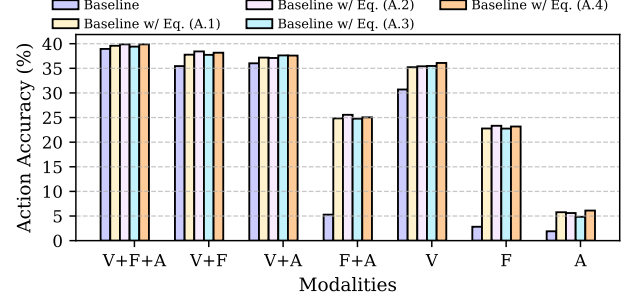


Figure 7. **Effectiveness of missing modality strategies across various modality combinations.** The “Baseline” uses the same architecture as our student (see Sec. 3.2) but is trained end-to-end with cross-entropy loss and without the KARMMA enhancements (see Sec. 3.4). When “Baseline” includes any of the strategies from Eqs. (5) to (8), it is also trained with 50 % modality dropout. “V,” “F,” and “A” refer to RGB video, optical flow, and audio, respectively.

Method	Average Acc. (%) $\uparrow$	Avg. Relative Drop (%) $\downarrow$	Average Rank $\downarrow$
Baseline	21.59	51.99	4.86
Baseline w/ Eq. (5)	29.02	31.13	2.86
Baseline w/ Eq. (6)	<u>29.33</u>	30.84	<u>2.00</u>
Baseline w/ Eq. (7)	28.95	30.98	3.14
Baseline w/ Eq. (8)	<b>29.44</b>	<b>30.53</b>	<b>1.57</b>

Table 7. **Summary of the effectiveness of missing modality strategies.** “Average Acc.” refers to the mean action accuracy across all modality combinations. “Avg. Relative Drop” indicates the mean relative accuracy drop compared to the full-modality setting (V+F+A). “Average Rank” is the mean rank across modality combinations. All values are derived from Fig. 7. Blue highlights the strategy used by our final student. **Bold** and underline values indicate the best and second-best results.

Fusion Approach	Noun Acc. (%)	Verb Acc. (%)	Action Acc. (%)
MBT [38]	<u>47.31</u>	<u>59.57</u>	<u>33.50</u>
Self-Attention	<b>47.88</b>	<b>61.45</b>	<b>34.99</b>

Table 8. **Comparison of fusion approaches.** All values are obtained using our teacher (see Sec. 3.2). Blue highlights the approach used in our final teacher and student. **Bold** and underline values indicate the best and second-best results.

Fig. 7 compares the effectiveness of the four missing modality strategies, while Tab. 7 summarizes the results using three metrics: average action accuracy, average relative drop compared to the full-modality setting (V+F+A), and average rank.

Learning  $k$  additional tokens per modality regardless of its presence (Eq. 7) results in the lowest average accuracy among all strategies. In contrast, replicating the learnable modality token (Eq. 6) significantly boosts accuracy and reduces the relative drop. However, the best results are

achieved by combining a single modality token with the  $k$  learnable tokens (Eq. 8), yielding a 7.85 % absolute gain in average accuracy (36.4 % relative) and a 21.46 % absolute reduction in relative drop (41.3 % relative) compared to using no strategy at all.

## B. Multimodal Fusion Approach

Since KARMMA is a multimodal framework, it must fuse features from multiple modalities. Tab. 8 compares the noun, verb, and action accuracy of our self-attention fusion approach (the transformer layers in the fusion block; see Sec. 3.2) with the Multimodal Bottleneck Transformer (MBT) [38], which uses five bottleneck tokens. Although MBT was designed for multimodal fusion, our self-attention approach outperforms it by 0.57 % in noun accuracy, 1.88 % in verb accuracy, and 1.49 % in action accuracy, corresponding to relative gains of 1.2 %, 3.2 %, and 4.4 %, respectively.

## C. [CLS] Token

Both our KARMMA teacher and student include a learnable [CLS] token in their fusion blocks, resulting in  $M + 1$  output tokens ( $M$  modality-averaged tokens and the [CLS] token) that passed to the multi-head MLP for action prediction (see Sec. 3.4). Fig. 8 shows how including the [CLS] token affects action accuracy across various modality combinations. Tab. 9 summarizes these results using three metrics: average action accuracy, average relative drop compared to the full-modality setting (V+F+A), and average rank.

Using both the  $M$  modality-averaged tokens and the [CLS] token yields the best results, with an absolute accuracy gain of 0.37 % (1.6 % relative) and a 1.61 % absolute reduction in relative drop (4.3 % relative) compared to using only the modality-averaged tokens. These results highlight that while the  $M$  modality tokens capture rich modality-specific information, the modality-agnostic [CLS] token captures valuable cross-modal information that boosts both accuracy and robustness to missing modalities.

## D. Generalization to Unseen Environments

Egocentric datasets are often biased toward the individuals who record them. To account for this, Epic-Kitchens [7] partitions its validation set into “Seen” participants (those who also appear in the training set) and “Unseen” participants (those who do not). The “Unseen” split is designed to evaluate model robustness to distribution shifts. Tab. 10 reports noun, verb and action accuracy of our student (see Sec. 3.2) on each split.

Accuracies on the “Unseen” subset are approximately 10% lower than on the “Seen” subset, highlighting the challenge of generalizing to new environments. Nevertheless,

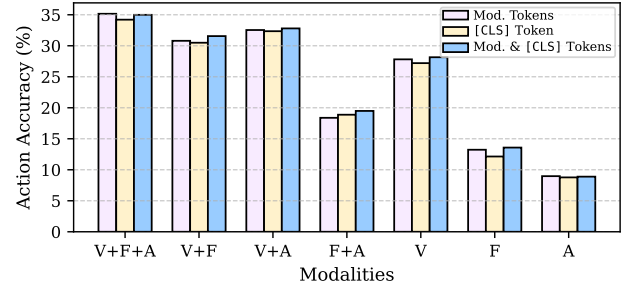


Figure 8. **Effect of the [CLS] token.** “Mod. Tokens” uses only the  $M$  modality-averaged tokens as input to the multi-head MLP (MH-MLP). “[CLS] Token” adds a [CLS] token to the fusion block and feeds only that token to the MH-MLP. “Mod. & [CLS] Tokens” uses both the  $M$  averaged modality tokens and the [CLS] token as input to the MH-MLP. Each bar shows the top-1 action recognition accuracy of our teacher (see Sec. 3.2). “V,” “F,” and “A” refer to RGB video, optical flow, and audio, respectively.

MH-MLP Input	Avg. Acc. (%) $\uparrow$	Avg. Rel. Drop (%) $\downarrow$	Avg. Rank $\downarrow$
Mod. Tokens	23.84	37.56	1.86
[CLS] Token	23.43	<u>36.75</u>	2.86
Mod. & [CLS] Tokens	<b>24.21</b>	<u>35.95</u>	<b>1.29</b>

Table 9. **Summary of the effect of the [CLS] token.** “Avg. Acc.” refers to the mean action accuracy across all modality combinations. “Avg. Rel. Drop” indicates the mean relative accuracy drop compared to the full-modality setting (V+F+A). “Avg. Rank” is the mean rank across modality combinations. All values are derived from Fig. 8. Blue highlights the MH-MLP input used in our final teacher and student. **Bold** and underline values indicate the best and second-best results.

Validation Set Split	Noun Acc. (%)	Verb Acc. (%)	Action Acc. (%)
Seen	<b>54.34</b>	<b>68.42</b>	<b>42.98</b>
Unseen	42.63	57.75	31.27
Seen & Unseen	<u>53.05</u>	<u>67.24</u>	<u>41.68</u>

Table 10. **Generalization of our student to unseen environments.** The validation set of Epic-Kitchens-100 [7] is divided into “Seen” and “Unseen” subsets: “Seen” contains data from participants present in the training data, while “Unseen” includes data from entirely new participants. “Seen & Unseen” refers to the full validation set. Blue highlights the validation split used in all experiments. **Bold** and underline values indicate the best and second-best results.

when evaluated on the full validation set (“Seen & Unseen”), the accuracy drop is smaller, indicating that our student retains a reasonable degree of robustness to participant-specific distribution shifts.

## E. Limitations

The main limitation of our proposed KARMMA framework is its reliance on transformer-based unimodal feature extractors, as the fusion block expects a sequence of  $k$  tokens per modality (with  $k$  potentially varying across modalities). Convolutional extractors, which output feature maps instead of token sequences, are therefore incompatible without additional adaptation. Furthermore, since our teacher relies on frozen pre-trained feature extractors, its accuracy depends on the availability of high-quality pre-trained models for each modality. Ideally, these extractors should be available in multiple sizes (*e.g.*, ViT-S and ViT-B), allowing the teacher to use a larger model while the student uses a smaller one, facilitating knowledge distillation by preserving architectural consistency.